

# Radiation measurement in Heliotron J

## by using an AXUV photodiode array with multiple optical filters

S. Watanabe, K. Nagasaki <sup>a</sup>, Y. Kowada, T. Mizuuchi <sup>a</sup>, H. Nishio <sup>b</sup>, H. Okada <sup>a</sup>, S. Kobayashi <sup>a</sup>,  
S. Yamamoto <sup>a</sup>, N. Tamura <sup>c</sup>, C. Suzuki <sup>c</sup>, K. Mukai, K. Hosaka, S. Mihara, H. Y. Lee, Y. Takabatake,  
S. Kishi, S. Konoshima <sup>a</sup>, K. Kondo, F. Sano <sup>a</sup>

*Graduate School of Energy Science, Kyoto University, Gokasho, Uji, Kyoto 611-0011, Japan*

<sup>a</sup> *Institute of Advanced Energy, Kyoto University, Gokasho, Uji, Kyoto 611-0011, Japan*

<sup>b</sup> *Department of Electronic Science and Engineering, Kyoto University, Kyoto, 606-8501, Japan*

<sup>c</sup> *National Institute for Fusion Science, 322-6 Oroshi-cho, Toki 509-5292, Japan*

The characteristics of spectrally-resolved plasma radiation with several heating methods have been investigated in Heliotron J by using an absolute extreme ultraviolet photodiode (AXUVD) array with multi-optical filters. Utilization of the multi-optical filters makes it possible to study the radiation characteristics separately in different photon energy ranges. For ECH and ECH+ICH plasmas at the density of  $0.3\text{-}0.4 \times 10^{19} \text{m}^{-3}$ , the radiation in the energy range of 20~70eV is dominant near the edge ( $\rho \sim 0.6\text{-}0.8$ ) region. The radiation increase in this energy range caused by the superposition of ICH to ECH qualitatively agrees with the increase of line emission from impurities such as C, O, Fe and Ti. For NBI plasma, the chord-integrated radiation for the photon energy ranges of  $\geq 200\text{eV}$  is more concentrated in the core region compared to that in ECH plasma. Comparison of different filtered data suggests that the radiation in the photon energy range of  $\sim 500\text{eV}$  is important for NBI plasmas.

Keywords: Heliotron J, AXUVD, radiation measurement, radiation profile, spectrally-resolved measurement

### 1. Introduction

Radiation from magnetically confined toroidal plasmas plays an important role in a power balance of the plasma and affects the accessible density limit. In order to investigate the radiation loss from the plasma, metal-foil bolometers and/or silicon photodiodes have been used in various fusion plasma experiments. Recently a wide-band silicon p-n junction photodiode has been developed by IRD, Inc., which is referred to as the absolute extreme ultraviolet photodiodes (AXUVD) [1]. AXUVD can measure the photon from visible to x-ray region (1.127eV to 100keV) due to the absence of a doped surface dead-region and zero surface recombination [1]. Other advantages of AXUVD are (1) fast time response and (2) insensitivity to long wavelength radiation like microwaves from the electron cyclotron heating system and (3) insensitivity to low-energy ( $< 500 \text{eV}$ ) neutral particles. Since the intensity of radiation from plasma depends on the photon energy (or wave-length) range, the energy spectrum must be studied for detailed investigation of the radiation characteristics. In order to measure the radiation in the vacuum ultraviolet (VUV) and soft X-ray region, a filtered AXUVD has been utilized [2, 3].

Recently an AXUD array system with multiple foil filters has been installed on Heliotron J. By using the filters the characteristics of radiation can be studied separately in

author's e-mail: w.shinya@center.iae.kyoto-u.ac.jp

the photon energy ranges. In this paper, we describe the characteristics of spectrally-resolved radiation from plasmas heated by different heating methods in Heliotron J.

### 2. AXUVD array system for Heliotron J

Heliotron J is a medium-sized helical-axis heliotron device ( $\langle R_0 \rangle = 1.2 \text{m}$ ,  $a = 0.1\text{-}0.2 \text{m}$ ,  $B_0 < 1.5 \text{T}$ ) with a low magnetic shear [4]. For plasma production and heating, second-harmonic X-mode ECH (70 GHz, 0.4 MW) [5], ICH (19-23.2 MHz, 0.6 MW) [6] and two tangential NBI (0.7 MW/beam-line, 30 kV H<sup>0</sup>-beam) [7] are applied.

Figure 1 shows the design of the AXUVD-array system. An aluminum plate of thickness  $50 \mu\text{m}^t$  with a slit of  $0.4\text{mm} \times 5\text{mm}$  is set in front of an AXUVD-array (AXUV16ELO/G, IRD, Inc.). The distance from the diode to the slit is 30 mm. The AXUVD array is set at a bottom port of Heliotron J and views the whole poloidal cross section as shown in Fig. 2. The viewing area of the center chord (ch-8) of the array, which views the plasma center, is  $32\text{mm} \times 146\text{mm}$  on the equatorial plane. The solid angle for this case is  $\sim 1 \times 10^{-5} \text{sr}$ . The diode current  $I$  is described by Eq. (1),

$$\frac{I}{S_{res} T_{trans}} = \int \int_{S_{obs}} \varepsilon \cdot \frac{\Omega}{4\pi} dS dl \quad (1)$$

Here  $S_{res}$  is the spectral responsivity in the diode,  $T_{trans}$  is

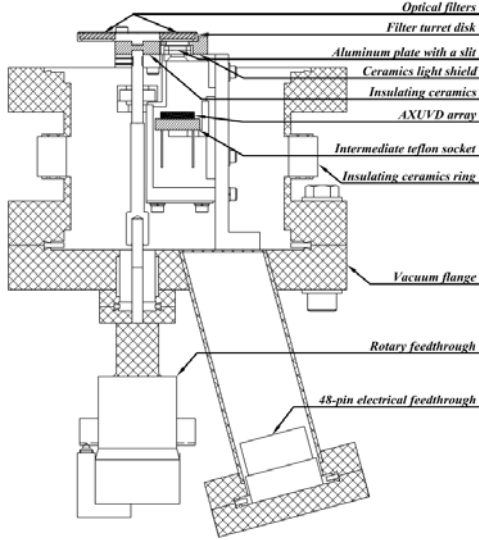


FIG. 1 The design of the AXUVD system.

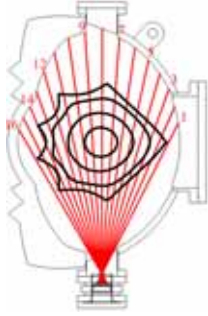


FIG. 2 The lines of sight of the AXUVD system (red) and magnetic flux surfaces (black).

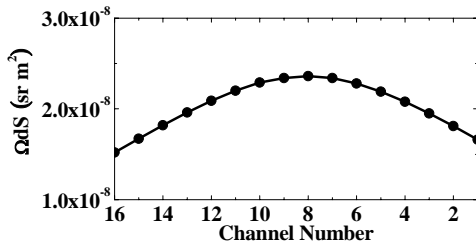


FIG. 3 Surface integral solid angle at each channel.

the transmittance of the optical filter,  $\varepsilon$  is the emissivity,  $S_{obs}$  is the observation area and  $\Omega$  is the solid angle for a small area of  $S_{obs}$ ,  $dS$ . Assuming that  $\varepsilon$  is constant on  $S_{obs}$ , the right part of Eq. (1) can be described by  $\int \varepsilon \int \Omega dS dl$ . When the distance from plasma to the diode is sufficiently longer than that from the slit to the diode,  $\int \Omega dS$  can be assumed to be constant along a line of sight. The value of  $\int \Omega dS$  at each channel is estimated as shown in Fig. 3. Then the  $\int \varepsilon dl$  can be obtained from the observed diode current by using Eq. (1).

As a filter system, two aluminum foils with thickness of  $1.0\mu m^t$  and  $0.2\mu m^t$  (tolerance  $\pm 10\%$ ), an interference filter (Al/LiF/Parylene) are mounted on a turret disk, located in front of the slit plane. The Al foils and the interference filter are supported by copper mesh

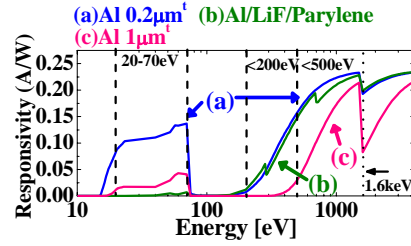


FIG. 4 Spectral responsivity of AXUVD with optical filters.

(a pitch of  $360\mu m$ , a mesh bar size of  $19\mu m$ ). The transmittance of the mesh can be estimated to be about 86% in the interesting energy range.

Figure 4 shows the spectral responsivities of the AXUVD with each filter, which are estimated by using the catalog data [8]. The application of the multi-optical filters makes it possible to estimate the radiated power in several separate photon energy ranges. The applications of the Al/LiF/Parylene and Al  $1\mu m^t$  filters can limit the effective sensitive photon energy range to  $\geq 200eV$  and  $\geq 500eV$ , respectively. Here, we set the lowest limit of the sensitive photon energy range as 10% of the maximum responsivity ( $\sim 0.24A/W$ ). On the other hand, the radiation in the photon energy band of 20~70eV can be estimated by subtracting the data measured with the Al  $0.2\mu m^t$  filter from those measured with Al/LiF/Parylene filter for identical discharges.

### 3. Radiation characteristics under different heating scenarios

#### 3.1 ECH+ICH plasma

Measurement of radiation for photon energy ranges of  $\geq 500eV$  and 20~70eV has been carried out for ECH plasma with the line-averaged density of  $0.3-0.4 \times 10^{19} m^{-3}$  for the standard (STD) Heliotron J configuration. In this experiment, a pulse of ICH ( $\sim 0.3MW$ ) is superposed on the ECH ( $\sim 0.35MW$ ) plasma.

Figure 5 shows an example of the time evolution of the line averaged density,  $\bar{n}_e$ , and the intensity of the AXUVD signals at center chord (ch-8),  $I_{AXUV}(ch-8)$ , for

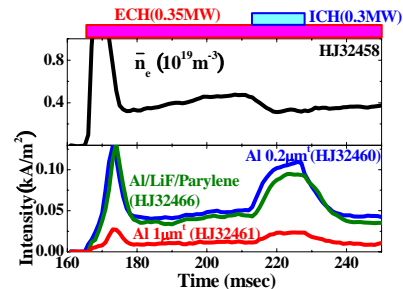


FIG. 5 Time evolution of the density and AXUV signals with different optical filters. An ICH pulse is superposed on ECH plasma during 213- 228ms.

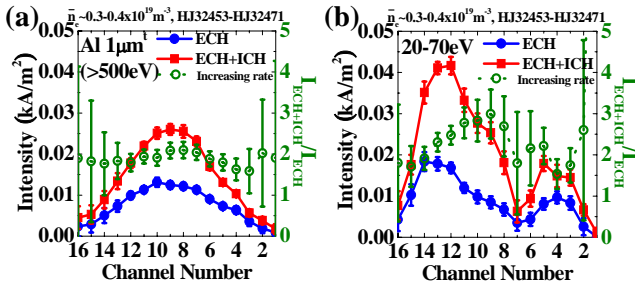


FIG. 6 The chord integral profiles of radiation in AXUVD with (a)  $1\mu\text{m}^{-1}$ -Al filter and (b) estimated energy of 20~70eV on ECH and ECH+ICH plasmas.

three filters cases. The signal intensity is increased for all the cases by the superposition of ICH, while  $\bar{n}_e$  is decreased slightly.

Figure 6 shows the chord-integrated profiles of the radiation for the photon energy range of (a)  $\geq 500\text{eV}$  and (b) 20~70eV. In the ECH plasma, the observed profile suggests that the radiation for the photon energy range of  $\geq 500\text{eV}$  is dominant near the plasma core, and that the radiation in the energy range of 20~70eV is dominant at the edge chords which are tangent to the surface near  $\rho \sim 0.6-0.8$  (chs-4, 13).

In the ECH+ICH phase, the signal intensity in each photon energy range is increased compared to those at the ECH-only phase. The ratio of  $I_{\text{AXUV}}$  at ECH+ICH phase to  $I_{\text{AXUV}}$  at ECH-only phase is also plotted in Figs. 6 (a) and (b). The increase ratios of the total intensities for the energy range of  $\geq 500\text{eV}$  and 20~70eV are about factors of 1.9 and 2.2, respectively. During the ICH superposition phase, it is observed that the line emission from impurities such as O, C, Ti and Fe are increased. Figure 7 shows the VUV spectra measured with a VUV polychromator for the ECH-only and ECH+ICH phases. Here, the observed wave-length range corresponds to the photon energy range of 32~73eV. This suggests that the increase of the line emission from the impurities might contribute to the increase of the radiation in the photon energy range of 20~70eV.

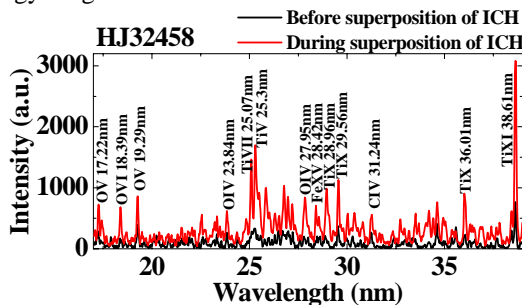


FIG. 7 VUV spectra in the range of 17-39nm (32-73eV) before and during the superposition of ICH to ECH plasma.

### 3.2 NBI plasma

The difference of radiation characteristics between ECH ( $\sim 0.35\text{MW}$ ) and NBI ( $\sim 0.35\text{MW}$ ) plasmas has been investigated at the density of  $0.9 \times 10^{19}\text{m}^{-3}$  under the STD configuration.

Figure 8 shows the time evolution of  $\bar{n}_e$ , the stored energy ( $W_p$ ),  $I_{\text{AXUV}}(\text{ch-8})$  with the  $1\mu\text{m}^{-1}$ -Al foil. The density and the stored energy increase after NBI and reach their maxima around  $t \sim 200-210\text{ms}$  and then are kept almost constant. On the other hand,  $I_{\text{AXUV}}(\text{ch-8})$  increases until  $t \sim 220\text{ms}$  and then it keeps a slightly lower level.

Figure 9 shows the difference in the  $I_{\text{AXUV}}$  profiles between ECH and NBI plasmas for the photon energy range of  $\geq 200\text{eV}$  and  $\geq 500\text{eV}$ . Here the time-averaged data at  $t = 230-250\text{ms}$  (the hatched phase in Fig. 8) are plotted. The  $I_{\text{AXUV}}$  profile in NBI plasma is centrally peaked compared to that in ECH plasma for both the energy ranges. The value of  $I_{\text{AXUV}}(\text{ch-8})$  is about five times higher than that for ECH plasma, while  $I_{\text{AXUV}}$  at ch-(1-5) and ch-(11-16) which correspond to  $\rho > 0.5$  is almost the same for both the ECH and NBI plasmas. The peaking factor of  $I_{\text{AXUV}}$  profiles, which is defined as the ratio of  $I_{\text{AXUV}}(\text{ch-8})$  to the total intensity for all channels, is also plotted in Fig. 8. It is shown that the peaking factor also continue to increase until  $t \sim 220\text{ms}$  and then is kept almost constant.

The total intensity in the photon energy range of

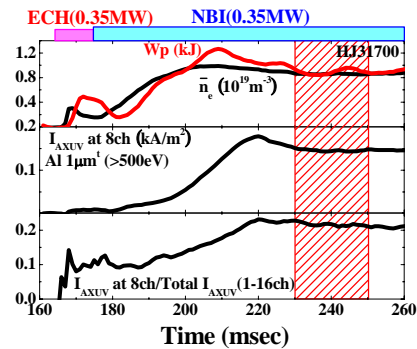


FIG. 8 Time evolution of  $\bar{n}_e$ ,  $W_p$ ,  $I_{\text{AXUV}}(\text{ch-8})$  with  $1\mu\text{m}^{-1}$ -Al filter and the peaking factor of the chord-integral radiation profile for NBI plasma.

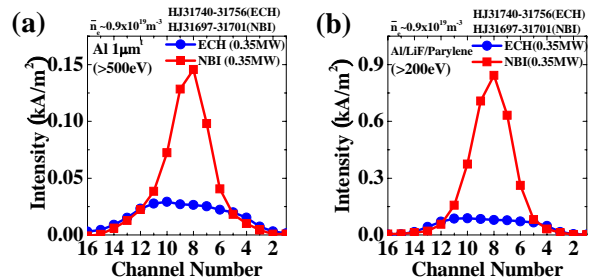


FIG. 9 The chord integral profiles of radiation measured with (a)  $1\mu\text{m}^{-1}$ -Al and (b) Al/LiF/Parylene filters on ECH and NBI plasmas.

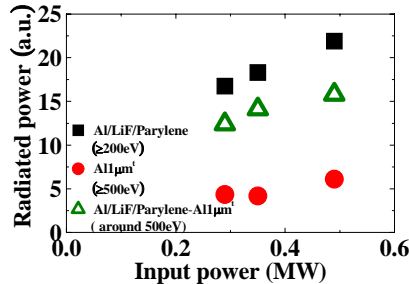


FIG. 10 The NBI power dependence of the radiated power measured with  $1\mu\text{m}^2$ -Al and with Al/LiF/Parylene filters by using averaged sensitivity.

$\geq 500\text{eV}$  is about 2 times higher for NBI plasmas compared to that for ECH plasma, while that in the energy range of  $\geq 200\text{eV}$  is about 4 times higher than that for ECH plasmas. On the other hand, the total intensity for all channels with Al/LiF/Parylene filter in NBI plasmas is about 5 times higher than that with the  $1\mu\text{m}^2$ -Al foil.

A difference of spectral responsivity between with Al  $1\mu\text{m}^2$  and with Al/LiF/Parylene filters arises in the photon energy ranges of  $\sim 500\text{eV}$  and  $\sim 1.6\text{keV}$  as shown in Fig.3. It is considered, however, that the difference of spectral responsivity in the energy range of  $\sim 1.6\text{keV}$  is not be important for this NBI data set since the pulse height analysis of the soft X-ray data for these plasmas indicate that the number of photons in the energy of  $\geq 1.6\text{keV}$  is a few orders smaller than that in the energy of  $\leq 1\text{keV}$ . In order to discuss the relative radiated power between different photon energy ranges, we estimate the “averaged sensitivity” for each sensitive energy range by averaging the spectral responsivity over the sensitive photon energy range; the averaged responsivity with Al/LiF/Parylene and Al- $1\mu\text{m}^2$  filters are  $0.18\text{A/W}$  ( $200\text{eV}\sim 1.5\text{keV}$ ) and  $0.15\text{A/W}$  ( $500\text{eV}\sim 1.5\text{keV}$ ), respectively.

Figure 10 shows the NBI power dependences of the total intensity for the data observed with  $1\mu\text{m}^2$ -Al and with Al/LiF/Parylene filters. The intensity is corrected by using the averaged sensitivity. The intensity increases with the NBI power. The intensity observed with the Al/LiF/Parylene filter (square symbol) is about 3-5 times higher than that observed with  $1\mu\text{m}^2$ -Al filter (circle symbol) for this NBI power range. Since the difference of the intensity come from the difference in the spectral responsivity shown in Fig. 3, the observation mentioned above suggests that the radiation from NBI plasmas might be dominated by that around  $500\text{eV}$ .

#### 4. Summary

The characteristics of spectrally-resolved radiation have been investigated for ECH, ECH+ICH and NBI

plasmas in Heliotron J by using AXUVD array with multi-optical filters. Utilization of the multi-optical filters makes it possible to study the radiation characteristics separately in different photon energy ranges.

For ECH and ECH+ICH plasmas at the density of  $0.3\text{-}0.4\times 10^{19}\text{m}^{-3}$ , the radiation in the photon energy range of  $20\sim 70\text{eV}$  is dominant near the edge ( $\rho\sim 0.6\text{-}0.8$ ) region. It is somewhat consistent with a general picture of the high temperature plasma radiation that the hollow profile with a large peak near the boundary consists of the low energy photons. The superposition of ICH to ECH plasma increases the radiation in the two photon energy ranges ( $20\sim 70\text{eV}$  and  $>500\text{eV}$ ). The increase in the  $20\sim 70\text{eV}$  range qualitatively agrees with the increase of line emission observed with the VUV polychromator from impurities such as C, O, Fe and Ti.

For NBI plasma, the  $I_{\text{AXUV}}$  profile is highly peaked compared to that in ECH plasma for the photon energy ranges of  $>200\text{eV}$ . The comparison of the data measured with  $1\mu\text{m}^2$ -Al to those with Al/LiF/Parylene filters suggests that the radiation from NBI plasmas might be dominated by the photons with the energy range around  $500\text{eV}$ . Although the source of the radiation increase has not been identified yet, the results indicate the importance of the radiated power in this energy range for the power balance analysis in the NBI plasmas.

The energy-resolved radiation monitor described in this paper would provide important information in plasma operation. An optical filter for the radiation of lower energy ( $<20\text{eV}$ ) will be set up in the next experimental campaign in order to extend the photon energy region.

#### Acknowledgements

The authors are grateful to the Heliotron J team for their excellent arrangement of the experiments. This work was partly supported by NIFS/NINS under the NIFS Collaborative Research Program (NIFS04KUHL005, NIFS07KUHL014).

#### References

- [1] Korde R et al., Metrologia **40** S145-S149 (2003)
- [2] Gray DS et al., Rev. Sci. Instrum. **75** 376 (2004)
- [3] Suzuki C et al., Rev. Sci. Instrum. **75** 4142 (2004)
- [4] Obiki T et al., Nucl. Fusion. **41** 833 (1999)
- [5] H. Shidara et al., Fusion Sci. Technol. **45**, 41 (2004)
- [6] H. Okada et al., Nucl. Fusion **47** 1346 (2007)
- [7] S. Kobayashi et al., 34th European Physical Society Conference on Plasma Physics, **P4-162** (2007)
- [8] <http://www.ird-inc.com/>